Proof-of-Principle Results for Identifying the Composition of Dust Particles and Volcanic Ash Samples through the Technique of Photon Activation Analysis at the IAC

Mayir Mamtimin,[a] Philip L. Cole,[a, b] and Christian Segebade[b]

[a]*Department of Physics, Idaho State University, 921 S. 8th Ave., Pocatello, Idaho 83209-8106*
[b]*Idaho Accelerator Center, 1500 Alvin Ricken Drive, Pocatello, Idaho 83201 (colephil@isu.edu)*

Abstract. Instrumental analytical methods are preferable in studying sub-milligram quantities of airborne particulates collected in dust filters. The multi-step analytical procedure used in treating samples through chemical separation can be quite complicated. Further, due to the minute masses of the airborne particulates collected on filters, such chemical treatment can easily lead to significant levels of contamination. Radio-analytical techniques, and in particular, activation analysis methods offer a far cleaner alternative. Activation methods require minimal sample preparation and provide sufficient sensitivity for detecting the vast majority of the elements throughout the periodic table. In this paper, we will give a general overview of the technique of photon activation analysis. We will show that by activating dust particles with 10- to 30-MeV bremsstrahlung photons, we can ascertain their elemental composition. The samples are embedded in dust-collection filters and are irradiated "as is" by these photons. The radioactivity of the photonuclear reaction products is measured with appropriate spectrometers and the respective analytes are quantified using multi-component calibration materials. We shall provide specific examples of identifying the elemental components of airborne dust particles and volcanic ash by making use of bremsstrahlung photons from an electron linear accelerator at the Idaho Accelerator Center in Pocatello, Idaho.
.

INTRODUCTION

Dust and ash can remain in the air for a quite long time, which can negatively impact the environment, and hence can impact human health. Industrial and agricultural waste is often dumped at sea or dumped in landfills and in the process heavy metals and other contaminants are released directly into the air. Further, volcanic eruptions will eject massive quantities of gases, ash, dust, molten lava, and will throw solid fragments into the air, where most of these spewed particles will eventually fall back to the ground by means of sedimentation [1]. We therefore need clear knowledge of the nature of these pollutants, with their relative elemental compositions, and we need a means for identifying the source of these particulates and for determining their pathways into and through the environment.

An important question arises concerning what exact kind of samples should be employed for extracting useful information on the air quality and ancillary environmental signatures. Given that different elements or chemical compounds characterize specific industrial processes, or even identify geographical locations, detailed studies of airborne particulates will give us a better understanding of the source and nature of changes to the environment. Wind, for example, can and will transport particulates globally. For the same reasons, studying volcanic ash makes for an excellent environmental sample, given that ash fallout is often responsible for sudden changes in local environment [2].   We seek a robust means to identify specific

elements, which is sensitive to the presence of trace elements at the μg/g (ppm) level, with the desirable feature of minimizing handling. Earlier elemental-analysis methods partially met these requirements of an automated instrumental analysis technique, which are sensitive to a wide range of elements [3]. In this paper we shall argue the case of the efficacy of Photon Activation Analysis for identifying elements in particulate matter.
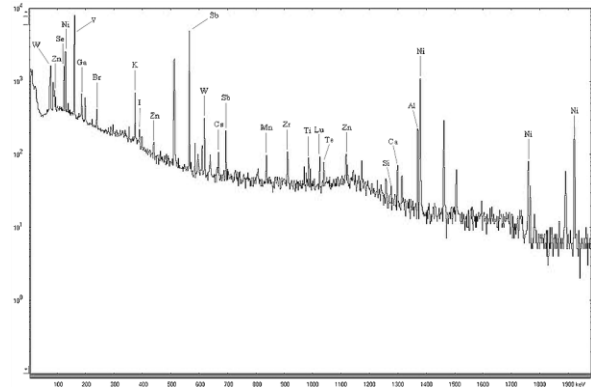
PHOTON ACTIVATION ANALYSIS

Photon Activation Analysis (PAA) is predicated on the physics of an energetic photon interacting with the nucleus. For example, when a photon of energy 15 MeV strikes a nucleus, a neutron can be liberated, and through these means, an excited, proton-rich nuclide is formed. That is, the photon activates this target nucleus. Complementary to PAA is the more commonly used technique of Neutron Activation Analysis (NAA). In the case of NAA, neutrons, instead of photons, activate the target nucleus [4,5]. However, NAA, if applied to the determination of trace quantities normally requires a nuclear reactor for generating the requisite neutron flux for proper activation, which is not altogether practical at most universities. Furthermore, frequently some restrictions have to be accounted for when using other activation techniques like 14 MeV NAA (small reaction cross sections; insufficient neutron flux) or charged particle activation (CPAA; analyses only the very outer surface of the item under study).

During photon activation analysis, nuclides of the analyte elements in the material samples are excited to radioactive nuclides. The high-energy photon interacts with the target nucleus and in the ensuing photonuclear reaction, a nucleon (proton or neutron) is ejected from the probed nucleus. Usually this nucleon is a neutron, as the Coulomb energy barrier will tend to inhibit protons from escaping. The resulting nuclide will be a proton-rich isotope of that interrogated element. In most cases, the isotope is unstable and this excited nuclide will decay by β^+ emission or electron capture (ε) to the lower Z isobar ususally through emitting several gamma rays, each having a characteristic energy ranging from ~100 keV to several MeV (see Fig. 1).
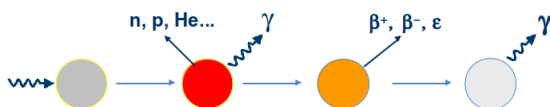
FIGURE 1. Photon Activation Analysis.

Measuring these discrete gamma rays will "fingerprint" the nuclide; the resulting characteristic spectral lines can then be identified with an appropriate spectrometer, such as a high-purity Germanium (HPGe) detector. And through the spectroscopy of identifying peaks within the complete gamma-energy spectrum, each chemical element – not the chemical species – can be detected qualitatively as is shown in Fig. 2. A thorough and detailed description of PAA can be found in reference [6].

Figure 2. Element-identified gamma peaks from irradiated dust samples collected in Santiago, Chile. The elements can be identified by the characteristic gamma decay energies, which "fingerprint" the particulates.

Photon activation analysis gives information on the type of element present within the sample. It cannot, however, determine the absolute number of nuclides activated. One cannot know *a priori* the exact mass of each of the separate elements within a random sample. Assuming uniform irradiation of the sample under interrogation, with all other beam parameters held fixed, the number of the proton-rich nuclides produced will scale with the absolute number of the interrogated isotopes of a specific element. Once the photon activation period is complete, the decay gamma rays from the excited nuclides are measured with a high-purity Germanium detector. And similarly a greater number of the photoproduced nuclides will be reflected by the higher intensities of the characteristic spectral signals, which are emitted from the proton-rich nuclides as they decay to ground state (Table 1). To determine the absolute masses of specific elements of the samples under scrutiny, a calibration material will have to be irradiated along with the interrogated sample. One usually employs a

TABLE 1. Analytically usable photonuclear reactions and calculated sensitivity

Z	Reaction	Half-life	E_γ[keV]	S [μg]
C	$^{12}C(\gamma, n)^{11}C$	20 min	511[a]	0.1
N	$^{14}N(\gamma, n)^{13}N$	9.96 min	511[a]	0.02
O	$^{16}O(\gamma, n)^{15}O$	2 min	511[a]	0.05
F	$^{19}F(\gamma, n)^{18}F$	110 min	511[a]	0.001
Cr	$^{52}Cr(\gamma, n)^{51}Cr$	27.8 d	320	0.3
Ni	$^{58}Ni(\gamma, n)^{57}Ni$	36 h	1379	0.06
As	$^{75}As(\gamma, n)^{74}As$	17.77 d	596	0.05
Zr	$^{90}Zr(\gamma, n)^{89}Zr$	78.4 h	909	0.03
Cd	$^{116}Cd(\gamma, n)^{115}C$ $^{115}Cd(\beta^-)^{115m}In$	53.38 h	336	0.05
Sb	$^{123}Sb(\gamma, n)^{122}Sb$	2.7 d	564	0.01
I	$^{127}I(\gamma, n)^{126}I$	12.8 d	388	0.04
Ce	$^{140}Ce(\gamma, n)^{139}Ce$	137.5 d	166	0.06
Tl	$^{203}Tl(\gamma, n)^{202}Tl$	12.2 d	440	0.04
Pb	$^{204}Pb(\gamma, n)^{203}Pb$	52.1 h	279	0.1
U	$^{238}U(\gamma, n)^{237}U$	6.75 d	59.5[b]	0.001

[a]after radiochemical separation
[b]to be measured by low energy photon spectroscopy

standard calibration material, where the elemental components are well known. After making the necessary spectroscopic measurements, we compare the spectra of the sample with that of the calibration material. We then can exactly determine the elemental make-up and thereby can ascertain the absolute concentration of specific elements present within the sample.

The primary advantage of this *in situ* method of PAA (sample with a calibrator) is that it can be carried out non-destructively. One does not need to specially prepare or machine the sample and hence there is a reduced danger of contamination from the debris of aggregated particles. And with this ease of handling, many more kinds of materials are open to investigation, especially materials, which are difficult to treat chemically, such as dust particles, fly ash, etc. Another advantage of PAA is its inherent high sensitivity. PAA has wide latitude of applications, ranging from the very small, i.e. minute mass, such as microgram dust particles, to the very big, i.e. massive multi-kilogram samples. As we are still very much in the developmental stage of this project, we will focus on our recent dust-particle assay results. Other

applications will surely come as we hone our analysis tools.

Discussion of the Method

At the Idaho Accelerator Center (IAC) in Pocatello, we have been conducting a series of proof-of-principle experiments on a variety of samples, ranging from air-borne dust particulates collected in Pocatello, Idaho [2], archival dust filters from Idaho National Laboratory Oversight Program to dust filters from Santiago, Chile, as well as volcanic ash obtained in southern Argentina from the summer 2011 eruption of Puyehue in Chile. Each of these samples was irradiated using the 44-MeV electron LINAC at the IAC. Further descriptions of applying the technique of PAA at the IAC can be found in Refs. [7,8,9,10].

Proper sample preparation is of prime concern in photon activation analysis for ensuring correct calibration and monitoring of the flux as well as measuring the transverse and axial flux gradient of the bremsstrahlung photon beam, which serves to irradiate both the sample and calibration materials simultaneously. For flux monitoring we may employ an internal monitoring scheme, where we add a well-known element (usually scandium or yttrium) mixed homogenously into both the sample and calibration materials. For external monitoring, we make use of nickel or copper foils upstream and downstream of the sample and calibration materials. To employ the internal monitor method, the samples should either be in powder or liquid form so that we may homogeneously add the monitoring element. Due to the special nature of our samples, however, we made use of only the external monitor scheme for our irradiated samples. Through this work, we are seeking to quantify the sensitivity of PAA in characterizing aerosol particulates and thereby identify trace elements in grain-sized matter, which we will quantify through mathematical modeling of the spectral peaks of the interrogated sample in direct comparison with those of the calibration material.

MATHEMATICAL MODELING OF THE SPECTRAL LINES

In this section, we briefly describe the mathematical means for extracting the concentration of elements. The method is described in detail in Ref. [11]. The original number of target nuclide in the sample is:

$$N_o = \frac{C_1 M A N_A}{A_r}. \qquad (1)$$

Here, C_1 is the concentration or the mass fraction of the target element in the sample, M is the mass of the sample, A is the natural abundance of the target nuclide, N_A is the Avogadro's constant, and A_r is the relative atomic mass.

When the sample is irradiated with high-energy photons within the energy regime of the Giant Dipole Resonance [12], the target nuclide will be activated with a characteristic transition rate of η. After an irradiation time period of t, the number of a specific daughter nuclide, reads:

$$N_2(t) = \frac{\eta N_o}{\lambda_2 - \eta}(e^{-\eta t} - e^{-\lambda_2 t}). \quad (2)$$

Here, each photoproduced daughter nuclide is specified with a decay parameter of λ_2, which is illustrated by the activity curve in Fig. 3.
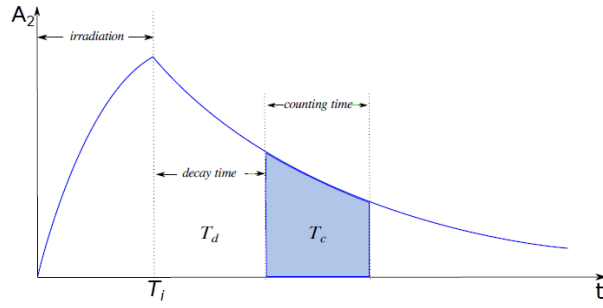

FIGURE 3. Activity curve.

In a real experiment, however, even though the operation time of an accelerator is several hours, the actual time of exposure is no more than a few 10s of seconds due to very low duty factor of a pulsed electron linear accelerator which, in our case at the Idaho Accelerator Center, turns out to be about 5×10^{-4} when operating at 240-Hz repetition rate and 2.3-μs pulse width. Under the nonrestrictive conditions that the number of original target nuclides in the sample stay constant, the transition factor η is negligible, and above equation becomes:

$$N_2(t) = \frac{\eta N_o}{\lambda_2}(1 - e^{-\lambda_2 t}). \quad (3)$$

During the irradiation of the sample for a time period (T_i), constant production of radioactive nuclides will give rise to the activity curve. The radioactivity of the activation product as a function of time (T_i, T_d) is defined by Eq. 4 (which is the general equation of nuclear activation; see also Fig. 3).

$$A_2(t)|_{t>T_i} = \frac{C_1 M A N_A}{A_r}(1 - e^{-\lambda_2 T_i})(e^{-\lambda_2 T_d})(\int_{E_{th}}^{E_{max}} \Phi(E) \cdot \sigma(E)dE), \quad (4)$$

where $\Phi(E)$ is the energy differential photon flux density and $\sigma(E)$ is the energy differential cross section.

After cooling the target for a period of T_d, we then count within the peak of the spectral lines arising from the decays of specific activated nuclides for a period of T_c with a HPGe detector. The concentration of target nuclide can be obtained using the total registered number of counts, which P_2 is the peak area as depicted in Fig. 4, counting efficiency of the detector (ε), and emission probability (p_λ).

$$C_1 = \frac{P_2 A_r \lambda_2}{M A N_A \varepsilon p_\lambda (1 - e^{-\lambda_2 T_i})(e^{-\lambda_2 T_d})(1 - e^{-\lambda_2 T_c})(\int_{E_{th}}^{E_{max}} \Phi(E) \cdot \sigma(E)dE)}. \quad (5)$$
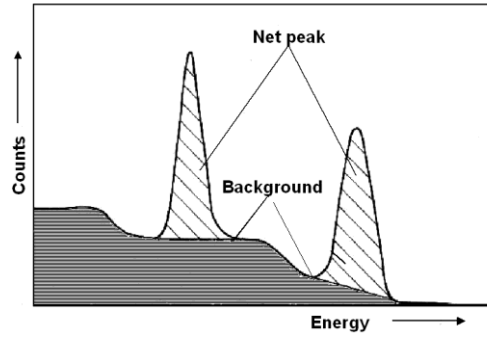

FIGURE 4. Net peak area of spectral lines.

We generally irradiate samples with a well-known calibration material and count with the same detector. That is to say, target nuclides exist in both the sample and the calibration material. And assuming that they go through the exact same photonuclear reactions under the same irradiation conditions, the concentration of target nuclides in the sample will be:

$$C_1^s = \frac{P_2^s A_r \lambda_2}{M^s A N_A \varepsilon p_\lambda (1 - e^{-\lambda_2 T_i})(e^{-\lambda_2 T_d^s})(1 - e^{-\lambda_2 T_c^s})(\int_{E_{th}}^{E_{max}} \Phi(E) \cdot \sigma(E)dE)}. \quad (6)$$

When the concentration of target nuclides in calibration material is:

$$C_1^r = \frac{P_2^r A_r \lambda_2}{M^r A N_A \varepsilon p_\lambda (1 - e^{-\lambda_2 T_i})(e^{-\lambda_2 T_d^r})(1 - e^{-\lambda_2 T_c^r})(\int_{E_{th}}^{E_{max}} \Phi(E) \cdot \sigma(E)dE)}. \quad (7)$$

We can then find the concentration of target nuclides with the aid of a well-known calibration material. That is to say, by taking the ratio of eqns. (6) and (7) and further introducing a flux correction factor, f_Φ, the equation for specific elemental concentration becomes:

$$C_1^s = f_\Phi \cdot C_1^r \, \frac{P_2^s M^r (e^{-\lambda_2 T_d^r})(1 - e^{-\lambda_2 T_c^r})}{P_2^r M^s (e^{-\lambda_2 T_d^s})(1 - e^{-\lambda_2 T_c^s})}. \qquad (8)$$

One of the conditions for the quantitative evaluation of the relative method is that both the sample and calibration materials should receive the same radiation dose, as the evaluation is performed by comparing the two resulting elemental spectra. The flux correction accounts for the radial and axial variations of the photon beam. To first order f_Φ is close to unity, but we are presently conducting Monte-Carlo simulations to further understand this systematic uncertainty.

SAMPLES AND RESULTS

Air Dust Samples

Preliminary results of one particular sample (Chilean air dust sample) are shown in Fig. 2, which shows the element-identified gamma energy lines. We then can identify the original nuclide with the concentration of that particular nuclide. The mass of dust collected on each sample ranges from 261 µg up to 1.5 mg. Samples were collected from two different locations and the period of dust collection spans one year. Elements common to all samples, with their corresponding weighted mean and uncertainty, are shown in Table 2.

TABLE 2. Elements and their concentration in air dust filters from Chile (µg/g).

| Z	4/5/00	7/26/00	12/21/00	3/15/01	4/11/01
Ca	3778±322	6080±804	5051±876	16588±5502	6155±365
Ti	525±84	631±109	811±224	7035±3337	774±131
	418±44	1158±101	880±335	525±158	1223±197
Br	517±73	484±102	658±106	168±61	351±123
Rb	21±7	15±5	21±8	8±3	44±18
Zr	16±5	20±4	17±4	15±5	20±7
Sb	16±2	22±3	12±3	14±5	13±3
Pb	312±37	355±27	286±64	132±20	148±38
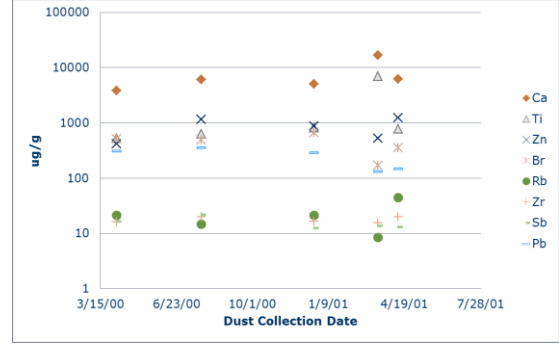
FIGURE 5. Trace element concentration change over time in air dust samples from Chile.

TABLE 3. Trace element concentration of volcanic ash samples (µg/g).

Z	6/4/2011	6/6/2011	6/15/2011	6/16/2011
Na	17716±2183	30597±4091	46836±9141	24471±3101
Mg	7458±702	10926±1084	6923±1617	4056±615
Ca	15879±1047	21513±1374	21878±1894	12281±720
Ti	3270±207	2665±235	5867±567	3716±232
Cr	6.6±1.7	9.4±2.8	13.7±6.6	8.4±3.3
Mn	373±50	682±99	724±147	418±59
Fe	18690±2250	38036±4808	34294±6040	26260±3219
Co	4.6±0.7	5.9±1.1	4.7±1.2	2.9±0.6
Zn	72±10	118±32	171±31	96±16
Ga	13±6	26±11	47±16	20±8
As	6.9±0.7	11.8±1.3	22±3.2	10±1.1
Rb	29±4	52±7	99±19	47±6
Sr	192±40	324±61	380±145	234±85
Y	24±2	43±5	68±10	36±4
Zr	135±18	248±35	452±91	221±30
Nb	3.8±0.6	7.8±1.4	11.5±2.5	5.8±0.9
Sn	10±1.5	8.5±1.9	25.4±6.7	7.5±1.8
Sb	3.5±0.5	6.2±2.6	10±1.7	4.2±0.9
I	1.3±0.2	3.3±0.6	4.6±0.9	2.5±0.4
Cs	1.7±0.3	3.2±0.5	5.9±1.3	2.9±0.4
Ba	527±202	707±295	930±366	732±227
Ce	24±4	43±7	73±16	36±6
Sm	5.2±1.3	4.7±0.8	7.9±2.3	4.9±1.2
Pb	9.3±1.7	15.9±4.1	27.1±5.7	15±3.4
U	0.6±0.2	1.1±0.3	2.1±0.6	1.1±0.3

By finding trace elements that are common in each sample during this period of one year, we can map the elemental change throughout this time period. After the analysis, we can see that certain elements group up at different concentration levels. Such as, calcium has the highest level of concentration; Rb, Zr, and Sb are in the group that has the lowest level of concentration; Ti, Zn, Br, and Pb group at the medium level. At the same time, we observe some tracking or anti-tracking patterns throughout the time period (Fig 5).

Other than these aforementioned common elements, many more elements were identified in each individual samples, again as indicated in Fig. 2. The low mass of the aggregated dust particles could be one of the reasons that some of these elements are not detectable in some samples. It is further conceivable that missing or spotty appearance of certain elements may be an indication of other complicated processes or reflects a plain meteorological process. Nevertheless, extremely low dust mass is one of the main reasons for poor statistics and detectability.
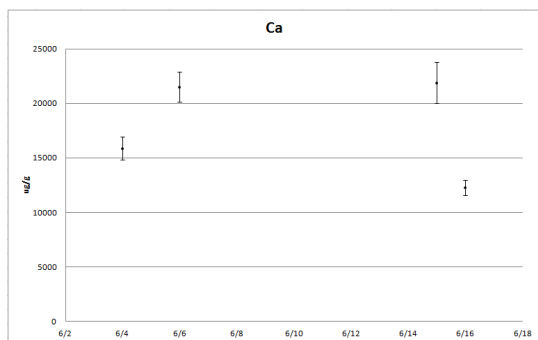
FIGURE 6. Concentration change for Ca over the two week span after the Puyehue eruption on June 4, 2011

Volcanic Ash

We have four separate volcanic ash samples, which were collected within the first two weeks of the Puyehue eruption of June 4, 2011 [13]. Samples were collected from the surrounding area of Puyehue National Park, which is very near the center of the eruption. These samples were prepared using the internal monitoring method as described above. And the trace element concentrations for each of these four samples are recorded in Table 3 with respect to the collection date. These elements provide key and fundamental information on the elemental make-up,

which clearly is of environmental interest. We observe that almost all the elements are less concentrated in samples, which were taken on June 4, 2011 and have higher concentration value for June 6 and June 15, followed by decreased concentration value on June 16, 2011. Figure 6 shows such a pattern for calcium as an example

Different periods could event stages such as continuous emission of ash at the beginning of the eruption, sedimentation process, evaporation, or environmental changes could well be the harbingers of such a pattern. In order to draw any further conclusions, one would need to repeat these experiments with a much larger number of samples and with more frequent collection dates.

SUMMARY AND PATH FORWARD

Photon Activation Analysis is proving to be an excellent method for investigating the elemental make-up of solid-particulate matter collected with air-dust filters. We have found that we are sensitive to grain masses much less than 250 μg. The technique of PAA, moreover, can be performed without having to chemically separate the components. There is just a minimum of sample preparation before and after the activation process. The overall sensitivity for low-mass material makes the method of PAA very promising for future environmental studies on airborne minute matter.

ACKNOWLEDGMENTS

REFERENCES

1. M. Z. Jacobson, *Atmospheric Pollution: History, Science, and Regulation*; Cambridge, New York, 2002.
2. Richard W. Boubel, Donald L. Fox, D. B. Tuner, Arthur C. Stern, *Fundamentals of Air Pollution*, 1994.
3. R. Dams, "Nuclear Activation Techniques for the Determination of Trace Elements in Atmospheric Aerosols, Particulates and Sludge Samples," *Pure and Appl. Chem.*, Vol. 64, No. 7, pp. 991-1014, 1992.
4. G. Hevesy and H. Levi, "The Action of Neutrons upon the Rare Earth Elements," *Mat.-Fys. Medd.*, 14, pp, 3-34, 1936.
5. R.R. Greenberg, P. Bode, and E.A. De Nadai Fernandes, "Neutron Activation Analysis: A Primary Method of Analysis," *Spectrochimica Acta Part B*, 66, 193-241 (2011).
6. C. R. Segebade, H. P. Weise, and G. J. Lutz, *Photon Activation Analysis*, Walter de Gruyter, Berlin, New York, 1988. ISBN: 3-11-007250-5
7. D.P. Wells, C.R. Segebade, and P.L. Cole, "Photon Activation Analysis at the Idaho Accelerator Center," AIP Conf. Proc. 1265 (2010).
8. M. Mamtimin, P.L. Cole, and C.R. Segebade, "Photon Activation Analysis of Dust Particles for Environmental Research and Applications using the 44-MeV Electron Linac at the Idaho Accelerator Center," *AIP Conference Proceedings for AccApp'11* (2012).
9. Z.J. Sun, D. P. Wells, C. R. Segebade, and J. Green, "Standardizing Activation Analysis: A New Software for Photon Activation Analysis," *AIP Conference Proceedings*, 1336(1), 473-478, 2011;
10. Z.J. Sun, "Photon Activation Analysis and Provenance Study of Coffee," *PhD Dissertation*, Idaho State University, Pocatello, 2012 *(unpublished)*.
11. M. Mamtimin, "Feasibility Study of Photon Activation Analysis on Airborne Particulates, Volcanic Ash, and Moon Dust Samples," *Master's Thesis*, Idaho State University, Pocatello, 2012 *(unpublished)*.
12. B.L. Berman and S. Fultz, "Measurements of the Giant Dipole Resonance with Monoenergetic Photons," *Reviews of Modern Physics*, 47, pp, 713-761, 1975.
13. *Puyehue Cordon Caulle Eruption.* (<http://en.wikipedia.org/wiki/2011> Puyehue-Cordon Caulle eruption)